Hindawi
Advances in Civil Engineering
Volume 2018, Article ID 7027432, 13 pages
https://doi.org/10.1155/2018/7027432

Research Article

Experimental and FEM Investigation of Cob Walls under Compression

Enrico Quagliarini[1] **and Gianluca Maracchini**[2]

[1]*Department of Construction, Civil Engineering and Architecture (DICEA), Università Politecnica delle Marche, Via Brecce Bianche, 60131 Ancona, Italy*
[2]*Department of Materials, Environmental Sciences and Urban Planning (SIMAU), Università Politecnica delle Marche, Via Brecce Bianche, 60131 Ancona, Italy*

Correspondence should be addressed to Enrico Quagliarini; e.quagliarini@univpm.it

Received 17 April 2018; Accepted 11 July 2018; Published 27 August 2018

Academic Editor: Damien Rangeard

Earth has been used as construction material since prehistoric times, and it is still utilized nowadays in both developed and developing countries. Heritage conservation purposes and its intrinsic environmental benefits have led researchers to investigate the mechanical behaviour of this material. However, while a lot of works concern with rammed earth, CEB, and adobe techniques, very few studies are directed towards cob, which is an alternative to the more diffused rammed earth and adobe in specific geographic conditions. Due to this lack, this paper presents an experimental program aimed at assessing the failure mode and the main mechanical properties of cob earth walls (compressive strength, Young's modulus, and Poisson's ratio) through monotonic axial compression tests. Results show that, if compared with CEB, adobe, and rammed earth, cob has the lowest compressive strength, the lowest modulus of elasticity, and Poisson's ratio. Differences are also found by comparing results with those obtained for other cob techniques, underlining both the high regional variability of cob and the need of performing more research on this topic. A strong dependence of material properties on loading rate and water content seems to exist too. Finally, the ability of a common analytical method used for masonry structures (an FEM macromodelling with a total strain rotating crack model) to represent the mechanical behaviour of cob walls is showed.

1. Introduction

Raw earth buildings constitute a considerable part of world cultural heritage. Examples can be found in different regions of the world, from the arid zones to the tropical and temperate latitudes [1–5]. About 15% of UNESCO heritage sites are built from raw earth [6], and it is estimated that about 30–40% of the world's population lives and works today in earthen architecture [7], owing to their qualities such as low cost, better thermal insulation, and use of local material. In the Marche region (Italy), about 245 earthen buildings are still present according to a recent census [8]. As these buildings are part of our cultural and architectural heritage and a testimony of low-environmental impact constructions, it is needed to preserve them from ruin and deterioration.

Damage to earthen structures can be caused by several environmental factors, mainly due to rainfall in combination with other factors or abandonment state [9–13]. These buildings are also characterized by a very low resistance against seismic lateral forces due to the low tensile and shear strengths of soil that in the past caused losses and casualties [3–5, 14–18]. Then, it is important to deepen the study on their mechanical performance, without which it is impossible to provide adequate retrofit interventions [19, 20].

Earthen construction can be divided into four main categories: compressed earth block (CEB), rammed earth, adobe, and cob construction. While a lot of studies were published on the mechanical behaviour of rammed earth, CEB, and adobe [7, 21–29], very few researchers studied the mechanical properties of cob, which constitutes a diffuse alternative to rammed earth and adobe in specific geographical

conditions [21, 30–33]. In fact, it is estimated that at least 200,000 units are constructed in EU by the cob technique, date back to the first half of the 20th century, the 19th century, the 18th century, and even older [30].

Cob technique consists in stacking wet clods (about cylindrical or ellipsoid heap) made of a mix of plastic earth often mixed with plant fibers to build load-bearing monolithic walls. In [30], a bibliographical analysis on cob processes is reported, attempting to take into account their regional variability. Concerning their mechanical behaviour, as already stated above, only few works can be found in the literature. In [31], the authors studied the compression and shear behaviour of still moist Italian cob walls (initial properties). However, no information was provided for walls in dried conditions. In [21], the mechanical behaviour of cob wall, characterized by a different clod preparation than that previously used in [31], was studied through both axial compression and diagonal compression tests. The authors found a more ductile behaviour than that of rammed earth and adobe [21]. In [33], cob walls of Pakistan were dynamically tested by using a shaking table in order to study the efficacy of a retrofitting solution based on vertical bamboos and horizontal plastic-coated steel wire mesh layers in improving the in-plane response of the walls. However, no information was provided about the construction process adopted.

In this work, an experimental program aimed at assessing the mechanical behaviour of the cob technique studied in [21], which is similar to other techniques adopted all around the world [30], is presented. In particular, the main mechanical properties of cob walls in dried condition such as compressive strength, Young's modulus, and Poisson's ratio, as well as the failure mode, are investigated through monotonic axial compression tests. In order to evaluate the effect on the results of a slower compaction phase before reaching failure, as may occur in real practice, the influence of the loading rate on mechanical behaviour was also investigated.

Mechanical properties of earthen materials strongly depend on water content too, as evidenced by the several studies focused on this topic [31, 34–37]. In [34], the authors showed that a slight increase in the moisture content of dry rammed earth is not followed by a sudden drop in strength. In [35], a strong dependence of the mechanical behaviour on the relative humidity at which the samples were stored was found. However, there are no studies for cob walls in this field. Due to this, a first insight into the relationship between water content and compressive strength and between water content and elastic modulus is also provided in this study.

Finally, since to the authors' knowledge, there are no research studies that address the analytical modelling of cob walls, the ability of an analytical method generally used for historic masonry (FEM macromodelling approach) to represent the mechanical behaviour of cob walls under compression is also investigated, that is, the smeared-crack approach (total strain crack model) [38].

2. Materials and Methods

2.1. Soil Type. In the past, builders, thanks to their experience and to the legacy orally transmitted by previous builders [39–41], had a specific knowledge on how to choose earth material for cob constructions. This knowledge is today partially lost in West countries, but it is still possible to learn from historic earthen buildings by means of geotechnical analyses [13, 30].

In this study, an earthen material that showed a good consistency with earth used in vernacular cob buildings (Figure 1) and that was adopted in previous works on cob [31, 42] was used. This material is also similar to that adopted in other studies on cob [13, 21]. Soil geotechnical data from testing are reported in Table 1 and Figure 2.

2.2. Construction Process of the Cob Walls. Four cob walls (Wall A, Wall B, Wall C, and Wall D) with average dimensions of $930 \times 310 \times 456\,\text{mm}^3$ ($L \times W \times H$) were made in a laboratory, following a cob construction technique developed over the centuries in the area of Macerata, Italy, as described in recent historic studies [31, 42]. Similar procedures were followed all around the world [13, 30].

The adopted process for the construction of a single cob element can be described as follows:

(i) Fragmenting the soil into small grains.

(ii) Mixing about 3 kg of soil (with an initial water content of 4.75%) and adding water until reaching the plastic consistency necessary for its workability (i.e., an average water content by weight of about 25–28% [31, 43]). A mechanical mixing machine commonly used in the manufacturing of fired-clay bricks was also used at this aim [31].

(iii) Shaping by hand by kneading until obtaining a cylindrical shape (diameter from 8 to 10 cm and a length of about 30 cm) [30, 31].

(iv) Rolling and pushing the earth cylinders on a wet straw-bed, so that the straw fibers, about 5–10 cm long, are present and adhere only on their external surface (Figure 3). In this way, substantially no straw fibers penetrate internally to the core of the cob element. This is consistent to what actually found in the vernacular cob wall buildings investigated in [31, 42] (Figure 1).

The water content of the cob elements at the end of the process was about 26.5%.

Cob walls were built by laying and pressing cob elements while they were still in a plastic state, with the longest side along the wall thickness and proceeding with staggered joints in successive layers (Figure 3). In this way, a layer of straw fibers separated each cob element from the others [42].

The dry density ρ_d of cob elements was estimated from intact specimens sampled according to [44]. An average ρ_d equal to $1.860\,\text{g/cm}^3$ was found, which is slightly higher than those found in the literature, which ranged from $1.400\,\text{g/cm}^3$ to $1.700\,\text{g/cm}^3$ [13, 21]. The walls were cured before testing for about two years at room relative humidity and temperature of the laboratory. The drying process was initially regulated by covering the walls with plastic sheets in order to limit the effect of shrinkage.

(a) (b)

Figure 1: (a) Typical raw earth cob architecture at the "Villa Ficana" district of Macerata, Italy; (b) cob elements constituting an existing wall.

Table 1: Geotechnical characterization of the soil used in this study.

	Soil used in this study
Gravel (>4.750 mm) (%)	0
Sand (0.075–4.750 mm) (%)	13.5
Silt (0.002–0.075 mm) (%)	50.5
Clay (<0.002 mm) (%)	36
Liquid limit (%)	42
Plastic limit (%)	21
Plastic index (%)	21
Water natural content (%)	22
USCS classification (%)	CL

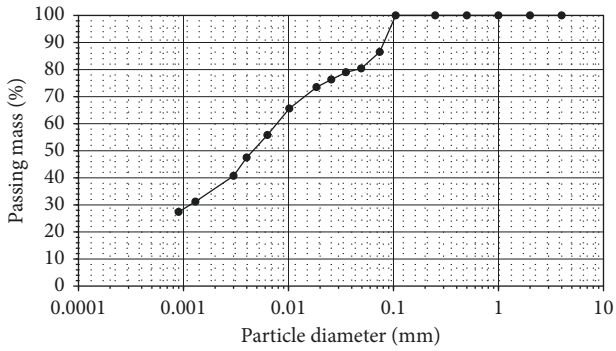

Figure 2: Grain size distribution of the adopted soil.

Since after the drying period the upper horizontal surfaces of the samples were not perfectly plane, mainly due to the presence of asperities, for each specimen, a rectification of the upper surface was obtained by filling asperities and voids with the plastic earthen material. Then, three loading-unloading cycles of about 5 kN of compression (i.e., about 0.03 MPa) were applied to ensure that the upper side of the sample was in contact with the plateau of the press, as also made in [34]. The applied loads were also useful to increase compaction in order to avoiding the occurrence of rigid dislocations of the elements in the early stages of the tests [43].

2.3. Axial Compression Test. The axial compression test consisted on applying a uniform distribution of vertical compression stresses on the upper horizontal side of the walls, that is, along the direction they generally withstood static loads. The tests were performed under force control with the test apparatus shown in Figure 4. In particular, two horizontal steel plates, adequately sprinkled with fat to reduce friction, were placed on the upper and lower sides of the specimens. The loading rate was defined in such a way to reach failure after about 15–20 min, as made in [21] (about 0.077 MPa/min). Moreover, in order to investigate the influence of the loading rate on the results, one specimen (Wall A) was tested by applying load at about one-third of the previous loading rate (about 0.025 MPa/min), in order to reach failure after about 50 min.

Four linear variable differential transducers (LVDTs) were used to monitor the vertical and horizontal deformations. Two horizontal LVDTs were placed on each specimen side while two vertical LVDTs were placed upon the steel plate, as depicted in Figure 4. The vertical/horizontal compression strains were then computed by averaging the measurements of the two vertical/horizontal LVDTs.

Finally, since mechanical properties of earthen materials strongly depend on water content [31, 34–37], the external and internal water contents of each wall (ω_i and ω_e, resp.) were calculated after testing according to [45] as mean of three values and then put in relation with the obtained compressive strengths f_c and the elastic modulus E. At this aim, six specimens were extracted for each tested wall, three from its external side and three from its core.

2.4. Numerical Modelling. The numerical modelling was carried out by using the FEM software MIDAS FEA [46] following a smeared-crack macromodelling approach in which the wall is treated as an homogeneous continuum medium. Despite the fact that cob walls could exhibit an anisotropic behaviour, an isotropic behaviour is here assumed due to the good consistency between numerical and experimental results, as it is usually done for other materials such as rammed earth [23] or masonry [47–49] that could exhibit anisotropic behaviour. In particular, the potentiality of the smeared-crack macromodelling approach to accurately simulate the mechanical behaviour of a rammed earth wall and to detect potential zones of failure by delamination has been recently shown in [23].

A 2D numerical model was created by using the averaged dimensions of the tested specimens, namely, $930 \times 310 \times 460\ \text{mm}^3$ ($W \times T \times H$). The 2D analysis represents

(a) (b)

Figure 3: Single cob element (a) and cob walls (b).

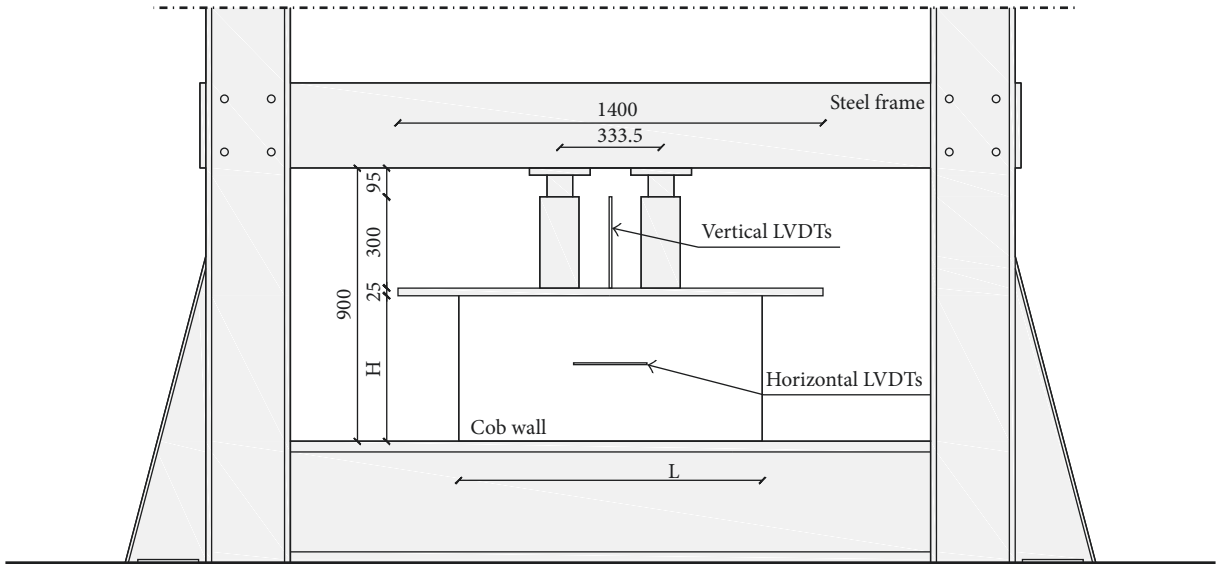

Figure 4: Test apparatus and LVDT placement for each specimen side (measures in millimeters).

a valid assumption given the geometry of the walls and the in-plane loading applied. A plane stress state was also assumed in order to reduce complexity and computer processing demand. Optimal mesh size was estimated through preliminary analyses. As a result, the adopted finite element mesh was constituted by 666 quadrilateral elements. A perfect confinement on the upper and lower surfaces was assumed as boundary conditions, as well as showed from compression test results. The load was applied as uniformly distributed vertical stresses on the upper edges of the constrained elements at the top of the model. A phased analysis was performed in order to consider the self-weight of the material.

For modelling the postelastic behaviour of the cob walls, an approach typically adopted for masonry materials was followed: crack opening was simulated through a total strain rotating crack model (TSRCM) that correspond to the modelling of distributed and rotating cracks based on total strain in which orthogonal cracks may develop in each integration point and the crack direction rotates with the principal strain axes [46]. In this way, although the interfaces between cob walls are not explicitly modelled, the localized cracking phenomenon is simulated in a disseminated way through the smeared-crack approach. A low tensile strength is assumed in order to simulate the low tensile strength of the interfaces. Several nonlinear stress-strain relationships can be used in this case according to the type of stress involved, that is, compression and tension. In this study, a parabolic relationship in compression and an exponential relationship in tension were initially adopted, as also made in [49] for the modelling of masonry and in [23] for the modelling of rammed earth (Figure 5).

In particular, the values of compressive strength (f_c), Young's modulus (E), and Poisson's ratio (ν) were obtained by averaging the results of the axial compression tests. Concerning Young's modulus, the progressive disappearance of voids, which results in a continuous variation during the test of the axial stiffness E, was taken into account in the model by using an averaged Young's modulus, representative of the first part of the curve during which voids disappear. In particular, this value was obtained by linear fitting the experimental load-displacement curves.

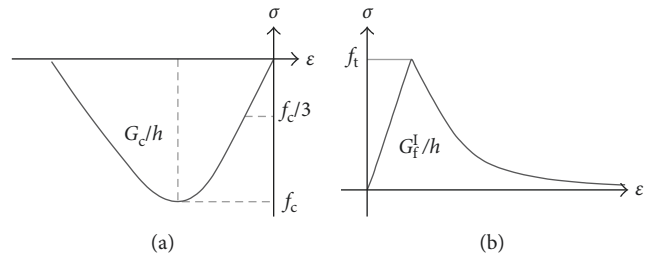

FIGURE 5: Stress-strain relationships adopted for the total strain rotating crack model: (a) compression; (b) tension.

The initial values of the compressive fracture energy (G_c) and the tensile strength (f_t) were estimated as $1.6 f_c$ and $0.1 f_c$, respectively, as recommended for historical masonry and as also made in [23] for the numerical modelling of rammed earth. As made in [23] for rammed earth, the mode-I tensile fracture energy G_f^I, instead, was set equal to $0.27\ f_t$, which is about 10 times than that usually assumed for masonry. This is due to the fact that, in the literature, cob walls and rammed earth walls seem to behave more as a monolithic material than historic masonry does, especially under compression stresses [23].

Finally, in order to make the results of the numerical analysis independent from the size of the finite element mesh, the crack band width (h) was assumed dependent on the area of the finite elements (A), that is, $h = \sqrt{A}$. A secant approach was used to simulate the unloading and reloading of the total strain rotating crack model.

3. Results and Discussion

3.1. Cob Wall Behaviour under Compression. Tests results of Walls B, C, and D are shown in Figures 6–8. In particular, the three experimental stress-strain curves (Figure 6) are very similar, highlighting the representativeness of the results. In the stress-strain curves, also the post-peak behaviour was reported (dotted lines in Figure 6), denoting a slight softening phase after reaching the compressive strength. However, since tests were carried out under force control, these experimental data cannot be considered as completely reliable. For this reason, this work was focused on the analyses of the pre-peak behaviour only.

On each experimental curve, three phases can be easily distinguished.

The first phase ends when the first capillary cracks were noticed, that is, at about 0.13 MPa or 1% of vertical strain ε_V (Figure 6). No notable horizontal deformations ε_H were recorded during this phase, probably due to the vertical compaction (i.e., filling of macrovoids) of the walls (Figure 7). This is a particular characteristic for the construction technique adopted since it means that, even after a manual compaction of the wall during the construction process and after the three precompression loading cycles of 0.03 MPa, some macrovoids between cob elements are still present and can be filled only with higher compression levels.

The elastic moduli and Poisson's ratio related to this phase (E_0 and ν_0, resp.) were computed by linear fitting the axial stress-strain curves (Figure 6) and the horizontal-vertical strain curves (Figure 7), respectively. The obtained values

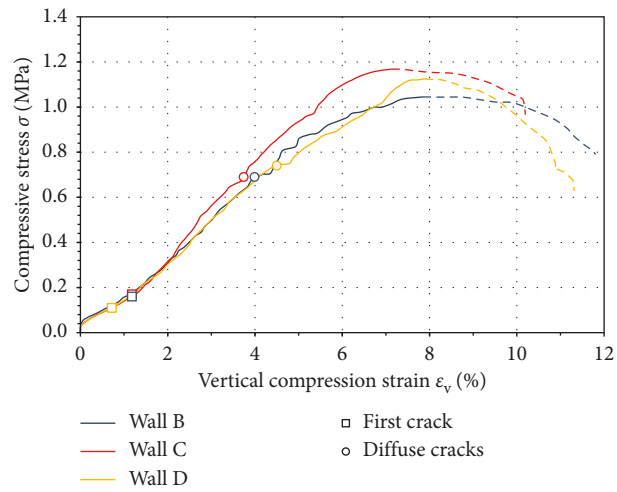

FIGURE 6: Compressive stress-strain diagrams for tested specimens. On each curve, the point related to the formation of the first capillary cracks and those related to the formation of diffuse cracks are reported. The vertical compression strains are computed by averaging the vertical displacements measured by the two vertical LVDTs. Post-peak behaviour (dotted lines) cannot be considered as completely reliable since test was force controlled.

are reported in Table 2 along with the related coefficient of variation (CV) and coefficient of regression (R^2). These latter are both useful to define the level of reliability of the obtained values.

In particular, the E_0 values are quite clustered (CV = 8.93%) but, due to the particular shape of the curve, the linear approximation does not seem particularly reliable ($R^2 = 0.70$–0.86). This is also evidenced by the very low values of R^2 (0.00–0.15) obtained for ν_0.

A first consideration can be drawn from this phase. In fact, since the compression stress coming from a single-storey earthen building is about 0.1 MPa [50], then, cob walls studied in this work are able to withstand common operating loads before cracking occurs.

The second phase is characterized by capillary cracks (the wall starts to be loaded as a whole, generating them), by the occurrence of the first notable horizontal strains ε_H (Figure 7) and by an upward concavity of the stress-strain curve (Figure 6).

Horizontal strains were due to the flattening of some cob elements and from the rigid dislocations of some others. This latter is caused by the mutual thrusts of elements under

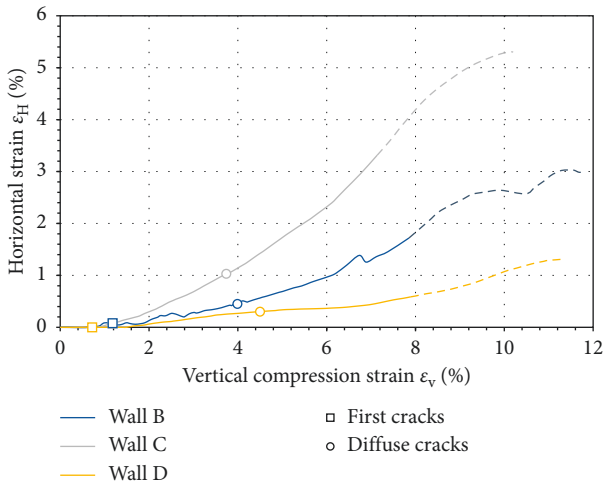

Figure 7: Horizontal strain-vertical strain diagrams for tested walls. On each curve, the point related to the formation of the first capillary cracks and those related to the formation of diffuse cracks are reported. The vertical and horizontal compression strains are computed by averaging the displacements measured by the two vertical and horizontal LVDTs, respectively. Post-peak behaviour (dotted lines) cannot be considered as completely reliable since test was force controlled.

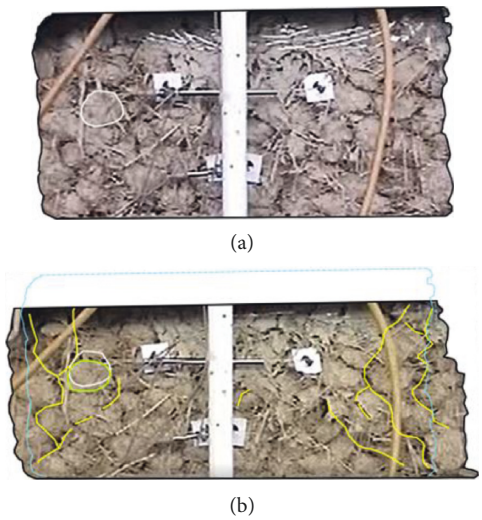

(a)

(b)

Figure 8: (a) Initial state and (b) typical crack pattern after the reaching of compressive strength. The flattening of a single cob element is also highlighted. Yellow lines: cracking; white line: undeformed shape of the cob element before testing; green line: deformed shape of the cob element after testing; blue dotted line: cob wall in undeformed shape.

compressive vertical stresses. In Figure 8, the deformation of a cob element during the test is highlighted.

The upward concavity of the stress-strain curve is caused by the gradual compaction of the cob elements which increases the global stiffness of the wall.

This phase ends when diffuse cracks started to be visible due to the reaching of the compressive strength in some cob elements, that is, at about 0.70 MPa and 4% of ε_V (Figure 6).

Table 2: For each specimen, elastic moduli and Poisson's ratio of the first and second phases, that is, E_0, ν_0 and E_1, ν_1, along with related mean values, coefficient of variation (CV), and range of coefficients of regression (R^2).

Sample ID	E_0 (MPa)	ν_0 (−)	E_1 (MPa)	ν_1 (−)
Wall B	16.17	0.05	16.56	0.15
Wall C	14.68	0.03	16.42	0.38
Wall D	17.56	0.00	17.75	0.10
Mean value	16.14	0.03	16.91	0.21
CV (%)	8.93	94.37	4.32	37.52
R^2_{range}	0.70–0.86	0.00–0.15	0.95–0.99	0.95–0.99

The elastic moduli and Poisson's ratios of the second phase (E_1 and ν_1, resp.) are reported in Table 2 along with the related CV and R^2. In this case, the linear approximation seems more reliable for both E_1 and ν_1 ($R^2 = 0.95$–0.99) than in the previous phase. However, while E_1 values are very clustered (CV = 4.32%), more scattered values were obtained for ν_1 (CV = 37.52%) as also evidenced in Figure 7. This is probably due to the random arrangement of the cob elements, which characterizes this construction technique and that lead to a different interlocking of the elements themselves.

The third phase is characterized by a strong nonlinear behaviour that ends with the reaching of the compressive strength f_c (about 1.12 MPa). After this, all the wallettes exhibited a brittle failure in a short time, and their failure is caused by the rigid dislocation of the external cob elements. Typical cone-shaped cracking pattern at the least on one side of the specimen (Figure 8) can be seen, whose extension depends on the friction generated between the steel plates and the specimen. As mentioned above, this is caused by the absence of horizontal joints and by the roundish shape of the cob elements. These factors, together, generate horizontal thrusts between each element inside the walls that pushed outwards the external elements once they exceeded the cohesion and friction forces developed at the interfaces between them. Due to the presence of the straw layer between cob elements, these surfaces constitute preferential fracture lines (Figure 8), where cohesion and friction forces are generally lower than those characterizing the earthen material.

3.2. Mechanical Parameters. Table 3 summarizes the single values, the mean values, and the scattering of the main mechanical properties obtained from compression tests.

Concerning the elastic parameters, our aim is to obtain E and ν values able to approximate in a simple manner the complex upward concave behaviour of the wall and that can be used in simple numerical modelling. At this aim, a correct definition of the elastic domain within which computing elastic moduli and Poisson's ratios is of fundamental importance.

In the literature, the elastic domain generally ranges between 0 and the stress value corresponding to a secant elastic modulus decrease of 20% than the initial modulus [51]. For concrete, for example, the modulus is the secant one measured between 0 and $0.4f_c$ [51]. For earthen materials

Table 3: For each specimen, compressive strength f_c and related strain ε_{fc}, elastic moduli and Poisson's ratio computed at 0.6 and $1/3f_c$ (E_{01}, ν_{01} and $E_{1/3}$, $\nu_{1/3}$, resp.), and mean internal and external water contents (ω_i and $\omega_{e,}$ resp.) are reported. The compression stresses related to the formation of the first capillary cracks (σ_1, end of the first phase) and those related to the formation of diffuse cracks (σ_2, end of the second phase) are also reported (Figure 6).

Sample ID	σ_1 (MPa)	σ_2 (MPa)	f_c (MPa)	ε_{fc} (%)	E_{01} (MPa)	$E_{1/3}$ (MPa)	ν_{01} (−)	$\nu_{1/3}$ (−)	ω_i (%)	ω_e (%)
Wall B	0.17	0.69	1.05	7.85	16.56	15.51	0.09	0.06	3.94	4.26
Wall C	0.16	0.68	1.17	7.14	17.72	15.51	0.21	0.13	5.03	4.54
Wall D	0.11	0.73	1.13	7.89	16.43	15.08	0.06	0.03	3.27	3.83
Mean value	0.15	0.70	1.12	7.63	16.90	15.37	0.12	0.07	4.08	4.21
CV (%)	21.92	3.28	5.47	5.53	4.20	1.62	66.14	69.98	21.77	8.49
R^2_{range}	—	—	—	—	0.97–0.99	0.97–0.99	0.93–0.94	0.57–0.81	—	—

including cob walls, the secant modulus was computed between 0.05 and $0.3f_c$ in [21]. In [34], a range between 0 and $0.2f_c$ was considered for rammed earth.

In our work, a decrease of 20% of the elastic modulus is hardly identifiable due to the particular shape of the curve (Figure 6). Then, two assumptions were made: the elastic moduli (E_{01}) and Poisson's ratios (ν_{01}) are computed between 0 and $0.6f_c$, that is, just before diffuse cracks occur; the elastic moduli ($E_{1/3}$) and Poisson's ratios ($\nu_{1/3}$) are computed between 0 and $1/3f_c$. As previously discussed, in both cases, a linear fitting of the axial stress-strain curves (Figure 6) and the horizontal-vertical strain curves (Figure 7) is performed to compute elastic moduli and Poisson's ratios, respectively.

For each assumption, in Table 3, the coefficient of variations CV and the ranges of the coefficients of regression R^2 are also reported, useful to provide an estimate of the reliability of the computed values.

Both the computed elastic moduli, that is, E_{01} and $E_{1/3}$, present a very low scattering (<5%) and high R^2 (>0.95), which highlights the reliability of the experimental results and of the linear approximation of the stress-strain relationship in this case.

Concerning Poisson's ratios, as expected a higher scattering was found. As discussed above, this is due to the construction technique adopted that, due to the random arrangement of the cob elements, leads to different interlocking between the cob elements, and different internal thrusts, for each wall tested under compression.

Since among the two ratios ν_{01} and $\nu_{1/3}$, the best linear fitting was obtained for ν_{01} ($R^2 = 0.93$–0.94), the elastic parameters E_{01} and ν_{01} were then considered as those that better represent the elastic behaviour of the walls for the numerical simulations.

In the following, the obtained results are compared with those reported in the literature for cob walls. At this point, it should be noted that a direct comparison with other results should carefully consider the different types of soil used.

However, some aspects of the mechanical behaviour are strictly related to the construction techniques adopted. Then, a meaningful comparison is still possible as long as these aspects are concerned.

In [21], even if a similar soil was adopted for cob walls, elastic moduli of tested cob walls present higher mean value and CV, 651 MPa and 68%, respectively, than those obtained in this study. Poisson's ratio was equal to 0.15 with a CV of 26%, which is quite similar to that obtained in our study (about 0.12 but with a higher CV). Concerning the compressive strength, similar values are obtained in other works [21] confirming that cob walls have the lowest compressive strength between earthen construction techniques. In particular, in [21], less scattered and slightly a higher mean value of f_c were obtained (CV = 1.9% and 1.59 MPa). Clearly, the compressive strength measured in this study could be partially affected by the aspect ratio (H/L) of the tested walls (about 0.5). In fact, it is known that a specimen characterized by a low aspect ratio generally provides higher results in terms of compressive strength than a slenderer one, due to the confinement effect caused by the friction between steel plates and the specimen. However, similar aspect ratios were used in the literature for earthen walls tested under compression [25, 31].

These differences, and in particular those related to the elastic parameters, which are the most relevant, can be attributable to the different preparation processes of cob elements. In fact, differently from what we did in our study, in [21], fibers were added within the kneading used for preparing cob elements, and no preferential fracture lines, such as those obtained in our study (straw layers between elements), can be distinguished in the wall. This had probably led to a more monolithic and stiffer behaviour than that obtained in our study.

Finally, concerning with the vertical strains corresponding to the compressive strength, ε_{fc}, a mean value of 7.63% was obtained which is higher than that obtained for rammed earth and adobe for which maximum ultimate vertical strain of 1% is usually obtained [21, 34].

3.3. Dependence of Mechanical Parameters on Loading Rate. Then, a fourth specimen (Wall A) was tested by applying a lower loading rate (0.025 MPa/min). Results in terms of compressive stress-strain diagrams and horizontal strain-vertical strain diagrams are reported in Figures 9 and 10 (Wall A-1) and compared to those obtained from the other walls.

Besides, in order to evaluate the residual compressive capacity after failure, an additional load (with the same loading rate) was applied to the same cracked wall. In fact, despite cracked, the wall was still intact after the first loading and might have a further resistance. In this case, the results are marked as Wall A-2 and reported in Figures 9 and 10.

The two stress-strain curves (Figure 9) are characterized by the same shape obtained for the other walls. Even the

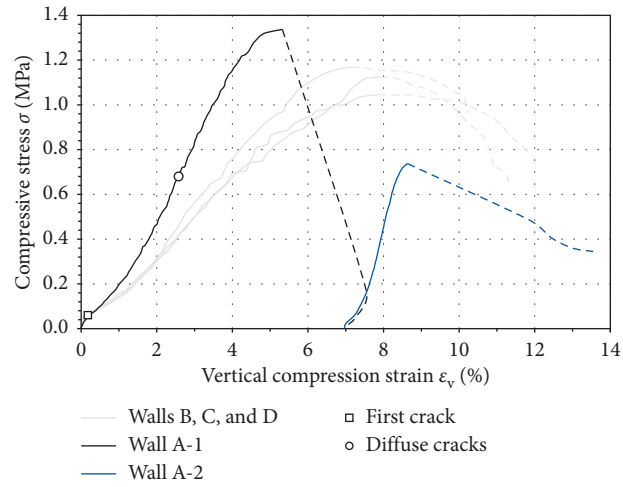

Figure 9: Compressive stress-strain diagrams for the specimen tested at about 0.025 MPa/min (Wall A) and comparison with other tested specimens (about 0.077 MPa/min). The reported vertical compression strains are obtained by averaging the displacements measured by the two vertical LVDTs, respectively. Post-peak behaviour (dotted lines) can be considered as completely reliable since test was force-controlled.

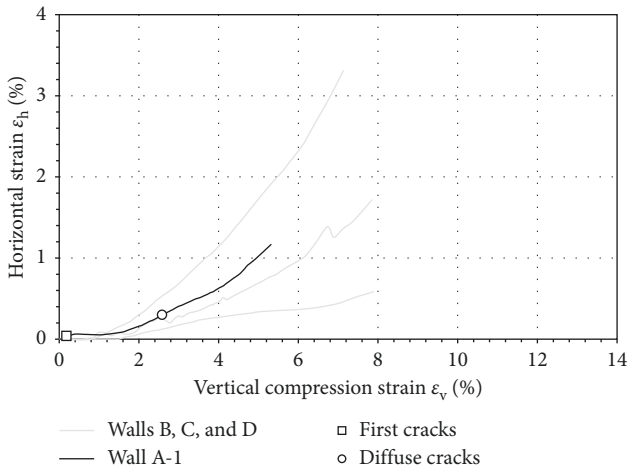

Figure 10: Horizontal strain-vertical strain diagrams for the specimen tested at about 0.025 MPa/min (Wall A) and comparison with other tested specimens (0.077 MPa/min). The reported vertical and horizontal strains are computed by averaging the displacements measured by the two vertical and horizontal LVDTs, respectively. Post-peak behaviour (dotted lines) can be considered as completely reliable since test was force controlled.

failure mechanism is the same observed for the other specimens, that is, the typical cone-shaped cracking pattern due to the rigid dislocations of cob elements seen in Figure 8. This means that these qualitative characteristics on the mechanical behaviour of cob walls under compression depend neither on the loading rate (Wall A-1) nor on the initial precompression of the specimen (Wall A-2).

The values of the mechanical parameters of Wall A-1 and Wall A-2 are reported in Table 4, along with the mean values obtained from the other tests where the effect of the different loading rate is highlighted. In particular, for Wall A-1, a higher elastic modulus E_{01} and a higher compressive strength f_c were obtained (1.4 and 1.2 times higher, resp., than the mean values previously obtained). This can be explained as follows. During loading, cob elements pass from a roundish shape to a more flattened one. Due to the lower loading rate, a better filling of voids is obtained before failure. As a result, on one hand, more friction between the external surfaces of the elements may be generated, which contrasts rigid dislocations and, consequently, increase global stiffness. On the other hand, due to the more flattened shape, a better distribution of the vertical compression stresses is provided between elements, lowering internal thrusts and delaying failure to higher f_c. Poisson's ratio (ν_{01}) seemed not particularly affected by the loading rate. The obtained value is in fact within the range of the scattered values obtained for the previous walls (Table 3).

The previous considerations were confirmed after the second loading, where the elastic modulus E_{01} obtained after the second loading (Wall A-2) was 1.45 times higher than the E_{01} obtained after the first loading. As expected, however, a decrease of the compressive strength is observed due to the loss of the cohesive bonds between elements in the previous phase.

3.4. Dependence of Mechanical Parameters on Moisture Content. The internal and external water contents (ω_i and ω_e, resp.) were measured (Table 3) and put in relation with both compressive strengths f_c (Figure 11) and elastic moduli E_{01} (Figure 12). In order to make a useful correlation, also the data collected in [31], related to still moist cob walls built with the same cob technique and the same soil type used in our study, have been reported in Figures 11 and 12. It should be noted that the cob walls tested in [31] are a little smaller than those tested in our study.

For each mechanical parameter, two different linear fitting curves were obtained, one for the external and one for the internal water contents. It should be noted that while the mechanical parameters are related to the entire section of the specimen, the water content is a local measure highly variable through the section for several days after the construction of an earthen wall (drying phase). Then, two different relationships were obtained due to the different values obtained for internal and external water contents in the drying phase. According to the literature [30], a maximum manufacture water content by weight of 25–30% is generally used for cob mixture around the world. Then, the adoption of linear fitting curves, which provide reasonable values of compressive strength and elastic modulus in the selected range of water content between about 0 and 25%, seems justified.

As expected, in any case, lower moisture levels correspond to higher compressive strengths and higher elastic moduli. For each mechanical parameter, the relationships related to internal water content (the blue ones in Figures 11 and 12) seem the most reliable to provide a first rough estimate of f_c and E_{01} values due to the higher values of R^2.

Table 4: Comparison between mechanical parameters obtained for Wall A tested at 0.025 MPa/min and mean values obtained from other specimens (0.077 MPa/min).

	σ_1 (MPa)	σ_2 (MPa)	f_c (MPa)	ε_{fc} (%)	E_{01} (MPa)	$E_{1/3}$ (MPa)	ν_{01} (−)	$\nu_{1/3}$ (−)	ω_i (%)	ω_e (%)
Mean BCD	0.15	0.70	1.12	7.63	16.90	15.37	0.12	0.07	4.08	4.21
Wall A-1	0.06	0.68	1.35	4.83	23.73	21.47	0.09	0.06	4.11	3.43
Wall A-2	—	—	0.74	1.66	34.68	30.21	—	—	4.11	3.43

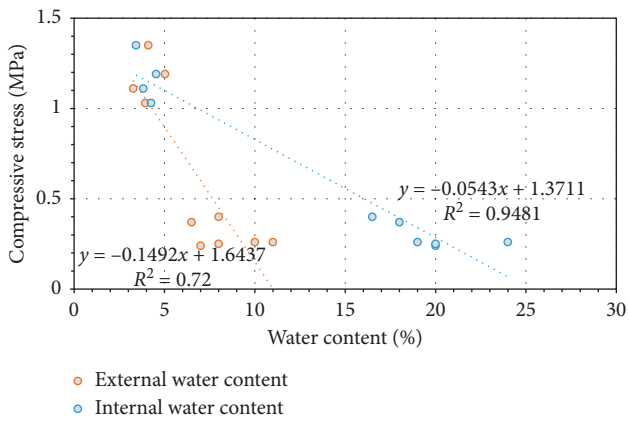

Figure 11: Dependence of compressive strength on internal and external water contents.

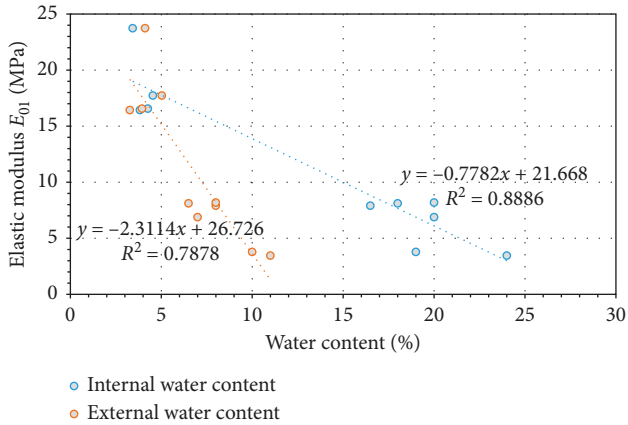

Figure 12: Dependence of elastic modulus on internal and external water contents.

This is mainly because the internal water content is more representative of the actual mechanical behaviour of the wall, especially during the drying phase. However, some more tests should be performed in order to obtain a higher level of reliability, even for other soil types [34].

After two years of drying, external and internal water contents have very similar values, ranging between 3 and 5%. This range can be considered as a typical range for both internal and external water contents of dried cob walls [30, 50]. Due to this, no meaningful differences between internal and external water contents were found in dried samples. Then, both could be used to provide a first estimate of the compressive strength and elastic modulus of dried samples from the blue relationships in Figures 11 and 12. This result is particularly important since it means that it is possible to obtain a first rough assessment of the compressive strength and elastic modulus of cob earthen buildings by using the external earthen material, that is, without invasive operations.

3.5. Numerical Analysis

3.5.1. Comparison between Numerical and Experimental Results. The initial values assumed for the mechanical parameters requested by the total strain rotating crack model (TSRCM) are reported in Table 5. In particular, the elastic parameters and the compression strength are computed by averaging the experimental values obtained from testing Walls B, C, and D.

The analytical stress-strain relationships obtained from these preliminary analyses are reported in Figure 13 along with the experimental curves.

The TSRCM model provides a good approximation of the experimental curve both in terms of stiffness and strength (Figure 13). This means that both the experimental values adopted as input for the numerical analysis and the shape of the constitutive laws are sufficient to represent with good approximation the cob behaviour under compression, at least for the pre-peak behaviour. However, it should be noted that if a more complex stress-strain curve has to be modelled, such as the experimental one obtained for the Wall A (Figure 9), a multilinear stress-strain relationship (with upward concavity) in compression should be adopted in order to adjust the pre-peak behaviour in terms of deformability.

The cracking pattern obtained from the model was also analyzed and compared with experimental ones (Figure 8). In particular, since a force-controlled analysis does not provide post-peak results, a displacement-controlled analysis was performed. At this aim, uniformly distributed vertical displacements were applied to the constrained nodes at the top of the model. Figure 14 presents the principal tensile strains and the plasticity status obtained for a vertical displacement ε_v of about 8%, that is, right after the compressive strength.

In the model, the higher tensile strains are concentrated in the lateral parts, due to the development of the typical cone-shaped damage pattern (Figure 14). This pattern corresponds to the system of cracks observed during the tests (Figure 8).

The model is then able to detect the zones that are more vulnerable to the occurrence of lateral rigid dislocations caused by the internal horizontal thrusts. However, as expected, the model does not catch the experimental rigid dislocation between cob elements due to the absence of

Table 5: Initial values for the mechanical parameters requested by the TSRCM.

E_{01} (MPa)	ν_{01} (−)	f_c (MPa)	G_c (N/mm)	f_t (MPa)	G_f^I (N/mm)
17.67	0.12	1.12	1.79	0.11	0.03

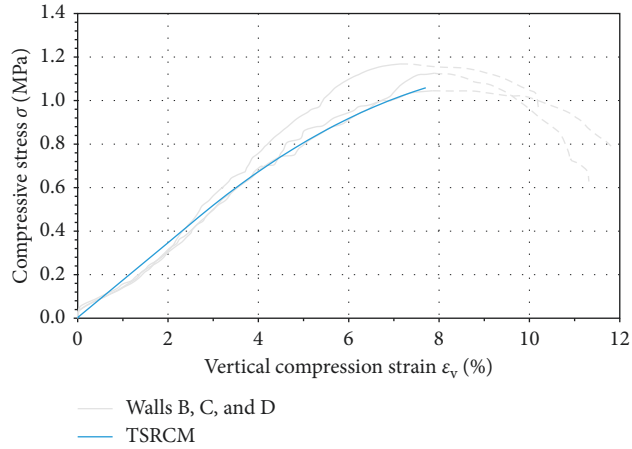

Figure 13: Comparison between TSRCM and experimental results in terms of stress-strain diagrams.

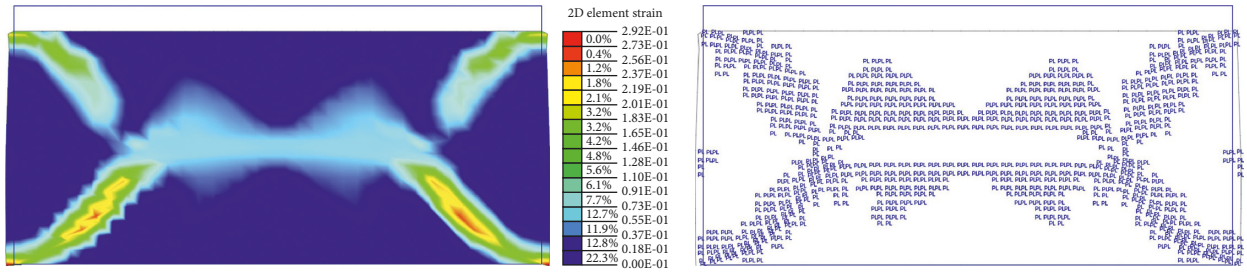

(a) (b)

Figure 14: (a) Principal tensile strains and (b) extent of plastic zones obtained for the displacement-controlled analyses for a vertical strain ε_v of about 8% (right after the reaching of the compressive strength).

interface elements. In this case, a micromodelling approach should be used.

3.5.2. Models Sensitivity on Poisson's Ratio. Among the different mechanical parameters obtained from experimental tests, Poisson's ratio presents the highest scattering and thence the highest uncertainty (Table 3). In order to evaluate the influence of this uncertainty on the numerical results, a sensitivity analysis of the model was then performed. At this aim, three values of Poisson's ratio were considered: a reference value $\nu_{ref} = 0.12$, an upper value $\nu_{upp} = 0.24$, and a lower value $\nu_{low} = 0.06$.

The results are reported in Figure 15 in terms of stress-strain diagrams where it can be noticed that the first linear part of the curve is not affected by the variation of the Poisson's ratio. Conversely, a higher influence of Poisson's ratio was found on the nonlinear part. In particular, the compressive strength and the related vertical strain ε_{fc} are inversely proportional to ν. However, the initial reference value ν_{ref} (i.e., that obtained experimentally) provided the best results. Then, it can be assumed as a first recommended value. However, further tests should be performed to validate this assumption in a statistical way.

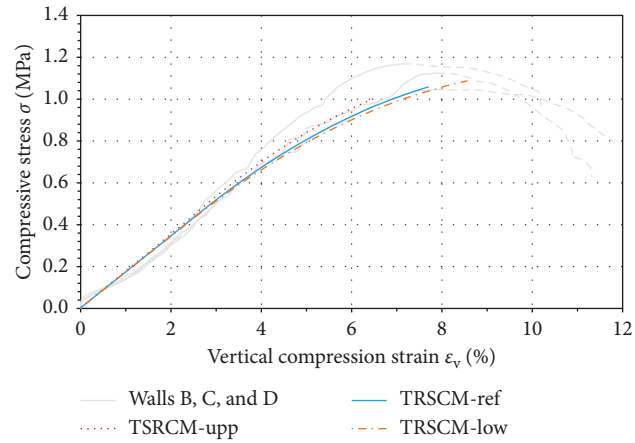

Figure 15: Influence of Poisson's ratio on the numerical results.

4. Conclusion

This paper deals with the experimental characterization and numerical simulation of cob walls under axial compression. In the first part, the axial compression test allowed characterizing important mechanical parameters such as compressive strength, elastic modulus, and Poisson's ratio. In order to do this, the elastic domain within which computing the elastic parameters was first estimated, that is, between 0 and $0.6f_c$ (just before diffuse cracks occur) for which a very good linear fitting was obtained. Then, a comparison between mechanical parameters and values from the literature was made. In particular, if compared with CEB, adobe, and rammed earth walls, the tested cob walls have the lowest compressive strength, modulus of elasticity, and Poisson's ratio. Even if compared with other cob techniques, in which the absence of discontinuities between cob elements led to a more monolithic behaviour [21], the cob walls studied in this work showed the lower mechanical properties, especially in terms of the stiffness values. Then, the high regional variability of cob techniques stressed in [30] was evidenced in terms of mechanical response, and the need of performing more tests on different techniques underlined.

Also the failure mode in compression was investigated. It occurred in a short time after reaching the compressive strength and was caused by the rigid dislocation of the external elements. Typical cone-shaped cracking pattern at least on one side of the specimen can be observed, whose extension depends on the friction generated between the steel plates and the specimen.

The influence of the loading rate on mechanical behaviour was also investigated in order to evaluate the effect on the results of a slower compaction phase before reaching failure, as may occur in real practice. In particular, by applying a lower loading rate, higher stiffness and higher strength values were obtained. This was probably due to the slower compaction that generates a higher flattening of the elements that, in turn, led to a higher increase of friction forces at the interfaces (due to a better filling of voids) and to a higher decrease of the internal horizontal thrusts (due to the better distribution of the vertical compression stresses) delaying the failure. Further studies should be carried out to deepen this aspect.

This is however consistent with the usual construction of cob walls in the past. After having built a wall with a height of 0.50–0.70 m, the successive layers of the cob were piled only after a drying period of some days [31, 42]. This permitted a slow compaction of the wall.

Useful linear relationships between internal/external water contents and compressive strength/elastic moduli were also provided. As expected, a higher correlation between internal water content and mechanical parameters was found. However, since in dry walls external and internal water contents are very similar, the external water content could be used to provide a first rough estimate of the mechanical parameters through the obtained relationships. In order to obtain a more precise estimate, however, further studies should be carried out even in this case.

In the second part of the paper, the ability of a common analytical approach to represent the observed nonlinear behaviour was investigated. In particular, the tested cob walls were modelled by considering a FEM macromodelling approach and a total strain rotating crack model (TSRCM). The experimental results were used as input parameters for the models while a sensitivity analysis on the most uncertain parameters (Poisson's ratio) was performed.

The numerical analysis provided good results both in terms of stress-strain curve and cracking pattern, at least for the pre-peak behaviour (towards our interest is oriented). In particular, the experimentally obtained values adopted for the requested mechanical parameters were sufficient to obtain a good representation of the experiment mechanical behaviour of the wall under compression and a model calibration were not needed.

The sensitivity analysis showed a high sensitivity of all the models on Poisson's ratio. This means that this parameter should be accurately estimated from experimental tests. From this study, a recommended value of 0.12, that is, that obtained experimentally and that provided the best simulation results, was suggested.

Finally, further tests should be performed to evaluate with more accuracy the parameters in tension and in shear.

Data Availability

The data used to support the findings of this study are available from the corresponding author upon request.

Conflicts of Interest

The authors declare that they have no conflicts of interest.

Acknowledgments

This research was performed as part of the employment of the authors at Università Politecnica delle Marche. The authors thank Professor Alessandro Stazi, who makes this research possible. In fact, all the single cob clods used to make the cob wall specimens come from the research "How to design conservative and retrofitting intervention on the Villa Ficana's raw earthen houses at Macerata (Italy)" (2005) sponsored by the Municipality of Macerata (Italy) (Department Resolution no. 2005/3/4.3), for which scientific responsibility was given to him. The authors also thank Professional Engineer Luigi Colombo, who helped in making the compression tests, and Professional Engineers Andrea Albertini, Michele Cingolani, and Gessica Romagnoli, who helped in making the cob walls.

References

[1] F. Pacheco-Torgal and S. Jalali, "Earth construction: lessons from the past for future eco-efficient construction," *Construction and Building Materials*, vol. 29, pp. 512–519, 2012.

[2] B. Bayizitlioğlu, "Conservation and maintenance of earth constructions: yesterday and today," *Historic Environment: Policy and Practice*, vol. 8, no. 4, pp. 323–354, 2017.

[3] M. Blondet and G. V. Garcia, "Earthquake resist ant earthen buildings?," in *Proceedings of 13th World Conference on*

Earthquake Engineering, Vancouver, BC, Canada, August 2004.

[4] M.I. Gomes, M. Lopes, and J. De Brito, "Seismic resistance of earth construction in Portugal," *Engineering Structures*, vol. 33, no. 3, pp. 932–941, 2011.

[5] M. M. Rafi, S. H. Lodi, H. Varum, and N. Alam, "Estimation of losses for adobe buildings in Pakistan," in *Proceedings of 15th World Conference on Earthquake Engineering (WCEE)*, Lisbon, Portugal, September 2012.

[6] UNESCO World Heritage Centre, *World Heritage List*, UNESCO, Paris, France, 2018, http://whc.unesco.org/en/list/.

[7] D. Torrealva, J. V. Neumann, and M. Blondet, "Earthquake resistant design criteria and testing of adobe buildings at Pontificia Universidad Católica del Perú," in *Proceedings of the Getty Seismic Adobe Project 2006 Colloquium*, pp. 3–10, Getty Conservation Institute, Los Angeles, CA, USA, 2009.

[8] F. Bravi and P. Cantillo, "Censimento e catalogazione," in *Dir. Reg. per IBeni Cult. e Paesaggistici Delle Marche. Archit. Di Terra Nelle Marche*, Tecnostampa, Recanati, Italy, pp. 45 –284, 2005, in Italian..

[9] M. Hall and Y. Djerbib, "Moisture ingress in rammed earth: part 1-the effect of soil particle size distribution on the rate of capillary suction," *Construction and Building Materials*, vol. 18, no. 4, pp. 269–280, 2004.

[10] M. Hall and Y. Djerbib, "Moisture ingress in rammed earth: part 2-the effect of soil particle-size distribution on the absorption of static pressure-driven water," *Construction and Building Materials*, vol. 20, no. 6, pp. 374–383, 2006.

[11] M. Hall and Y. Djerbib, "Moisture ingress in rammed earth: part 3-sorptivity, surface receptiveness and surface inflow velocity," *Construction and Building Materials*, vol. 20, no. 6, pp. 384–395, 2006.

[12] M. Bertagnin, *Architetture di Terra in Italia*, Edicom Edizioni, Monfalcone, Italy, 1999, in Italian.

[13] F. Stazi, A. Nacci, F. Tittarelli, E. Pasqualini, and P. Munafò, "An experimental study on earth plasters for earthen building protection: the effects of different admixtures and surface treatments," *Journal of Cultural Heritage*, vol. 17, pp. 27–41, 2016.

[14] United Nations Office for the Coordination of Humanitarian Affairs (UNOCHA), *Balochistan Earthquake 2013 Findings and Strategies*, UNOCHA, New York, NY, USA, 2013.

[15] A. S. Arya and T. Boen, "Earthquake resistant construction of earthen housing," in *Proceedings of International Workshop Earthen Buildings in Seismic Areas*, pp. 1–18, Albuquerque, NM, USA, May 1981.

[16] M. Ahmadizadeh and H. Shakib, "On the December 26, 2003, southeastern Iran earthquake in Bam region," *Engineering Structures*, vol. 26, no. 8, pp. 1055–1070.

[17] Y. Calayır, E. Sayın, and B. Yön, "Performance of structures in the rural area during the March 8, 2010 Elazığ-Kovancılar earthquake," *Natural Hazards*, vol. 61, no. 2, pp. 703–717.

[18] M. M. Rafi, S. H. Lodi, M. Ahmed, and N. Alam, "Observed damages in Pakistan due to 16 April 2013 Iran earthquake," *Bulletin of Earthquake Engineering*, vol. 13, no. 2, pp. 703–724, 2014.

[19] J. Vargas, J. Bariola, M. Blondet, and P. K. Mehta, "Seismic strength of adobe masonry," *Materials and Structures*, vol. 19, no. 4, pp. 253–258, 1986.

[20] M. C. J. Delgado and I. C. Guerrero, "Earth building in Spain," *Construction and Building Materials*, vol. 20, no. 9, pp. 679–690, 2006.

[21] L. Miccoli, U. Müller, and P. Fontana, "Mechanical behaviour of earthen materials: a comparison between earth block masonry, rammed earth and cob," *Construction and Building Materials*, vol. 61, pp. 327–339, 2014.

[22] L. Miccoli, A. Drougkas, and U. Müller, "In-plane behaviour of rammed earth under cyclic loading: experimental testing and finite element modelling," *Engineering Structures*, vol. 125, pp. 144–152, 2016.

[23] L. Miccoli, D. V. Oliveira, R. A. Silva, U. Muller, and L. Schueremans, "Static behaviour of rammed earth: experimental testing and finite element modelling," *Materials and Structures*, vol. 48, no. 10, pp. 3443–3456, 2015.

[24] L. Miccoli, A. Garofano, P. Fontana, and U. Müller, "Experimental testing and finite element modelling of earth block masonry," *Engineering Structures*, vol. 104, pp. 80–94, 2015.

[25] E. Quagliarini, S. Lenci, and M. Iorio, "Mechanical properties of adobe walls in a Roman Republican domus at Suasa," *Journal of Cultural Heritage*, vol. 11, no. 2, pp. 130–137, 2010.

[26] P. Jaquin, C. Augarde, and C. Gerrard, "Historic rammed earth structures in Spain, construction techniques and a preliminary classification," in *Proceedings of International Symposium on Earthen Structures 2007*, Interline Publishing, Bangalore, India, August 2007.

[27] T. T. Bui, Q. B. Bui, A. Limam, and J. C. Morel, "Modeling rammed earth wall using discrete element method," *Continuum Mechanics and Thermodynamics*, vol. 28, no. 1-2, pp. 523–538, 2016.

[28] E. Quagliarini, M. D'Orazio, and S. Lenci, "The properties and durability of adobe earth-based masonry blocks," in *Eco-Efficient Mason Bricks Blocks*, pp. 361–378, Elsevier, New York, NY,USA, 2015.

[29] E. Quagliarini and S. Lenci, "The influence of natural stabilizers and natural fibres on the mechanical properties of ancient Roman adobe bricks," *Journal of Cultural Heritage*, vol. 11, no. 3, pp. 309–314, 2010.

[30] E. Hamard, B. Cazacliu, A. Razakamanantsoa, and J. C. Morel, "Cob, a vernacular earth construction process in the context of modern sustainable building," *Building and Environment*, vol. 106, pp. 103–119, 2016.

[31] E. Quagliarini, A. Stazi, E. Pasqualini, and E. Fratalocchi, "Cob Construction in Italy: some lessons from the past," *Sustainability*, vol. 2, no. 10, pp. 3291–3308, 2010.

[32] V. G. Kondekar, O. R. Jaiswal, and L. M. Gupta, "Optimization of Gadhi soil mix for adobe brick," *Electronic Journal of Geotechnical Engineering*, vol. 20, pp. 3965–3972, 2015.

[33] M. M. Rafi and S. H. Lodi, "Comparison of dynamic behaviours of retrofitted and unretrofitted cob material walls," *Bulletin of Earthquake Engineering*, vol. 15, no. 9, pp. 3855–3869, 2017.

[34] Q.-B. Bui, J.-C. Morel, S. Hans, and P. Walker, "Effect of moisture content on the mechanical characteristics of rammed earth," *Construction and Building Materials*, vol. 54, pp. 163–169, 2014.

[35] F. Champiré, A. Fabbri, J. C. Morel, H. Wong, and F. McGregor, "Impact of relative humidity on the mechanical behavior of compacted earth as a building material," *Construction and Building Materials*, vol. 110, pp. 70–78, 2016.

[36] P. Gerard, M. Mahdad, A. Robert McCormack, and B. François, "A unified failure criterion for unstabilized rammed earth materials upon varying relative humidity conditions," *Construction and Building Materials*, vol. 95, pp. 437–447, 2015.

[37] B. François, L. Palazon, and P. Gerard, "Structural behaviour of unstabilized rammed earth constructions submitted to

hygroscopic conditions," *Construction and Building Materials*, vol. 155, pp. 164–175, 2017.

[38] D. D. C. C. Drucker and W. Prager, "Soil mechanics and plastic analysis or limit design," *Quarterly of Applied Mathematics*, vol. 10, no. 2, pp. 157–165, 1952.

[39] L. Keefe, *Earth Building-Methods and Materials, Repair and Conservation*, Taylor and Francis Group, Abingdon, UK, 2005, https://books.google.lu/books?id=odt_agaaqbaj.

[40] J. McCann, *Clay and Cob Building*, Shire Publications, London, UK, 1995, https://books.google.it/books/about/clay_and_cob_buildings.html?id=pzhppgaacaaj&redir_esc=y.

[41] I. I. Akinwumi, P. O. Awoyera, and O. O. Bello, "Indigenous earth building construction technology in Ota, Nigeria," *Indian Journal of Traditional Knowledge*, vol. 14, no. 2, pp. 206–212, 2015.

[42] E. Quagliarini, E. Fratalocchi, and E. Pasqualini, "Caratterizzazione della terra che costituisce le case," in *Archit. Terra a Maceratail Quart. Di Villa Ficana. Anal. Conoscitiva per Recuper*, E. Quagliarini and C. Tassi, Eds., pp. 99–119, Alinea Editrice, Firenze, Italy, 2008.

[43] C. H. Kouakou and J. C. Morel, "Strength and elasto-plastic properties of non-industrial building materials manufactured with clay as a natural binder," *Applied Clay Science*, vol. 44, no. 1-2, pp. 27–34, 2009.

[44] ASTM International, *ASTM D7263–09 Standard Test Methods for Laboratory Determination of Density (Unit Weight) of Soil Specimens*, ASTM International, West Conshohocken, PA, USA, 2009.

[45] ASTM International, *ASTM D 2216-10 Standard Test Methods for Laboratory Determination of Water (Moisture) Content of Soil and Rock by Mass*, ASTM International, West Conshohocken, PA, USA, 2010.

[46] Midas FEA, Analysis and Algorithm Manual, 2006.

[47] E. Quagliarini, G. Maracchini, and F. Clementi, "Uses and limits of the equivalent frame model on existing unreinforced masonry buildings for assessing their seismic risk: a review," *Journal of Building Engineering*, vol. 10, pp. 166–182, 2017.

[48] F. Clementi, V. Gazzani, M. Poiani, P. A. Mezzapelle, and S. Lenci, "Seismic assessment of a monumental building through nonlinear analyses of a 3D solid model," *Journal of Earthquake Engineering*, pp. 1–27, 2017.

[49] G. Bartoli, M. Betti, P. Biagini et al., "Epistemic uncertainties in structural modeling: a blind benchmark for seismic assessment of slender masonry towers," *Journal of Performance of Constructed Facilities*, vol. 31, no. 5, pp. 1–18, 2017.

[50] H. Houben and H. Guillaud, *Earth Construction : A Comprehensive Guide*, CRAterre, Intermediate Technology Publications, London, UK, 1994, https://books.google.it/books/about/earth_construction.html?id=yjvsaaaamaaj&source=kp_cover&redir_esc=y.

[51] CEN, *Eurocode 2-Design of Concrete Structures Part 1-1: General Rules and Rules for Buildings-EN 1992-1-1*, European Committee for Standardisation (CEN), Brussels, Belgium, 2005.